Diffuse alveolar damage and thrombotic microangiopathy are the main histopathological findings in lung tissue biopsy samples of COVID-19 patients

Farahnaz Sadegh Beigee [a], Mihan Pourabdollah Toutkaboni [b,*], Neda Khalili [c,1], Seyed Alireza Nadji [d,1], Atosa Dorudinia [b,1], Mitra Rezaei [d,1], Elham Askari [b,1], Behrooz Farzanegan [e], Majid Marjani [f], Amir Rafiezadeh [b]

[a] Lung Transplantation Research Center, National Research Institute of Tuberculosis and Lung Diseases (NRITLD), Shahid Beheshti University of Medical Sciences, Tehran, Iran
[b] Chronic Respiratory Diseases Research Center, National Research Institute of Tuberculosis and Lung Diseases (NRITLD), Shahid Beheshti University of Medical Sciences, Tehran, Iran
[c] School of Medicine, Tehran University of Medical Sciences, Tehran, Iran
[d] Virology Research Center, National Research Institute of Tuberculosis and Lung Diseases (NRITLD), Shahid Beheshti University of Medical Sciences, Tehran, Iran
[e] Tracheal Diseases Research Center, Masih Daneshvari Hospital, Shahid Beheshti University of Medical Sciences, Tehran, Iran
[f] Clinical Tuberculosis and Epidemiology Research Center, National Research Institute of Tuberculosis and Lung Diseases (NRITLD), Masih Daneshvari Hospital, Shahid Beheshti University of Medical Sciences, Tehran, Iran

ARTICLE INFO

ABSTRACT

Background: Since the outbreak of the novel coronavirus disease-2019 (COVID-19) in December 2019, limited studies have investigated the histopathologic findings of patients infected with severe acute respiratory syndrome coronavirus-2 (SARS-CoV-2).
Material and methods: This study was conducted on 31 deceased patients who were hospitalized for COVID-19 in a tertiary hospital in Tehran, Iran. A total of 52 postmortem tissue biopsy samples were obtained from the lungs and liver of decedents. Clinical characteristics, laboratory data, and microscopic features were evaluated. Reverse transcription polymerase chain reaction (RT-PCR) assay for SARS-CoV-2 was performed on specimens obtained from nasopharyngeal swabs and tissue biopsies.
Results: The median age of deceased patients was 66 years (range, 30–87 years) and 25 decedents (81 %) were male. The average interval from symptom onset to death was 13 days (range, 6–34 days). On histopathologic examination of the lung specimens, diffuse alveolar damage and thrombotic microangiopathy were the most common findings (80 % and 60 %, respectively). Liver specimens mainly showed macrovesicular steatosis, portal lymphoplasmacytic inflammation and passive congestion. No definitive viral inclusions were observed in any of the specimens. In addition, 92 % of lung tissue samples tested positive for SARS-CoV-2 by RT-PCR.
Conclusions: Further studies are needed to investigate whether SARS-CoV-2 causes direct cytopathic changes in various organs of the human body.

1. Introduction

As of August 9th, 2020, approximately 19 million confirmed cases of coronavirus disease-2019 (COVID-19) have been reported worldwide as well as more than 722000 deaths [1]. Previous studies have shown that

severe cases of COVID-19 may develop acute respiratory distress syndrome (ARDS), multiple organ failure, and ultimately succumb to death [2,3]. Among patients with COVID-19, older individuals, male patients, and those with comorbidities are known to have higher morbidity and mortality rates [4,5][38]. Respiratory failure seems to be the main cause

---

* Corresponding author at: Department of Pathology, Chronic Respiratory Diseases Research Center, Masih Daneshvari Hospital, Shahid Beheshti University of Medical Sciences, Tehran, Iran.
E-mail address: pourabdollah@sbmu.ac.ir (M. Pourabdollah Toutkaboni).
[1] Authors contributed equally.

of death in infected patients [6]; identification of the exact mechanism of death, however, can only be achieved after performing pathologic examination on decedents.

COVID-19 is thought to involve many organs of the human body, including the lungs, heart, brain, liver, and kidneys among others [7–10]. Since December 2019, many studies discussed the clinical and radiological characteristics of COVID-19; nonetheless, information regarding the extent of this systemic disease on postmortem biopsies and/or autopsies is limited. Preliminary reports from China showed that the dominant histopathologic change in the lungs of infected patients was diffuse alveolar damage [11], a finding that was also reported on computed tomography (CT) imaging of patients with COVID-19 [12] [39]. Due to safety precautions and the challenges associated with performing autopsy on deceased patients infected with this novel and relatively unknown coronavirus, few studies have investigated the postmortem histopathologic findings of patients infected with SARS-CoV-2 so far. In this study, we report the histopathologic findings of deceased patients with COVID-19 in whom tissue samples were obtained from the lungs and the liver.

2. Material and methods

In this study, 31 deceased patients who were hospitalized for COVID-19 were randomly selected. All patients had been admitted to a tertiary care hospital in Tehran, Iran between March 2020 and April 2020. Postmortem tissue biopsy samples were obtained from the lungs and liver of decedents. In 24 cases, blind biopsy sampling of the lung tissue was performed through a 2-centimeter incision centered over the anterior axillary line within the sixth intercostal space of the right hemithorax. In one case, after a limited thoracoabdominal incision was made, the inferior lobe of the right lung, and a wedge-shaped sample of the liver were excised. In addition, blind biopsy sampling of the liver tissue was performed in 26 cases through a subcostal incision on the midclavicular line. Curved forceps was used for all of the surgical sampling procedures.

All of the obtained samples were then transferred to separate containers and were fixed with 10 % buffered formalin. Samples were kept at room temperature for 10 days before being transferred to the pathology ward for further processing. Representative sections were stained with hematoxylin and eosin (H&E), Masson trichrome, periodic acid-Schiff (PAS), Gram, Ziehl-Neelsen and Gomori methenamine silver, and were reviewed by at least two pathologists independently. Nucleic acid was extracted from the lysed tissue sections with the QiaSymphony system (QIAGEN, Hilden, Germany) and SARS-CoV-2 RNA was detected based on the sequence described by Corman et al. [13]. On histologic examination, the presence of hyaline membranes was considered as the sine qua non of diffuse alveolar damage, and other pathological features were used to determine the stage of diffuse alveolar damage.

All tissue biopsies were obtained with the consent of decedents' next of kin. This study was approved by the ethics committee of Shahid Beheshti University of Medical Sciences.

3. Results

3.1. Demographic data, clinical and laboratory characteristics

Among a total of 31 deceased patients, 25 patients (81 %) were male. The median age of patients was 66 years (range, 30–87 years); four patients were smokers and two other patients had quit smoking five and two years earlier. Different underlying comorbidities were found among deceased patients; the most common comorbidity was hypertension followed by diabetes [12 (38 %) and 10 (32 %) patients, respectively]. Also, one patient (3 %) had recently received chemotherapy for ovarian cancer therapy. With respect to initial presenting symptoms, the most frequent symptoms among patients were fever and cough [11 (35 %) and 6 (19 %) patients, respectively]. However, all patients had

developed dyspnea, fever, and cough by the time of admission.

At admission, the median oxygen saturation was 78 % on room air (range, 58 %–91 %). Two patients had suffered from out-of-hospital cardiac arrest before admission, and two patients had already been intubated prior to referral to our center. The median interval from symptom onset to admission was 7 days (range, 3–18 days), and the median interval from admission to intubation was 3 days (range, 0–15 days). In addition, the average time from symptom onset to death was 13 days (range, 6–34 days). Postmortem interval (from death to biopsy) varied from 1 to 7 h.

All patients had undergone chest x-rays and CT scans; but, due to the critical condition of patients, repeat chest CT was only performed in two patients at our center. After reviewing patients' medical records, all patients had extensive bilateral lung involvement on imaging (Fig. 1).

As shown in Table 1, laboratory examinations showed low lymphocyte and eosinophil values, reduced albumin, mildly elevated liver enzymes, and increased levels of ferritin, lactate dehydrogenase and erythrocyte sedimentation rate. In terms of coagulation function, although prothrombin time, international normalized ratio, D-dimer and fibrinogen levels were frequently elevated, partial thromboplastin time did not show a markedly elevation.

3.2. Results of reverse transcription polymerase chain reaction (RT-PCR) assay

Results of antemortem RT-PCR assay for SARS-CoV-2 obtained from nasopharyngeal swabs were positive in all but three patients (90 %). In these RT-PCR negative patients, diagnosis of COVID-19 was made based on compatible clinical and radiological findings.

From 25 lung tissue samples, 23 samples tested positive for SARS-CoV-2 by RT-PCR. Among liver tissue samples, 10/27 had a positive RT-PCR result, including three patients with liver biopsies as the sole provided specimen. In addition, in the three mentioned patients with negative nasopharyngeal swabs, positive RT-PCR results were found on lung tissue samples, with one case showing a concomitant positive RT-PCR on liver tissue sample (Table 2).

3.3. Tissue biopsy specimenssample

A total of 52 postmortem tissue biopsy samples were collected, including 26 liver tissue specimens (ranging in size from 0.6 to 1 cm), 24 lung tissue specimens (ranging in size from 1 to 5 cm), one wedge-shaped liver specimen (3.3 × 1.7 × 0.7 cm), and one lower pulmonary lobe specimen (14 × 12 × 8 cm). As mentioned earlier, the latter two specimens were obtained from one of the decedents through a thoracoabdominal incision.

3.4. Microscopic findings

3.4.1. Lung

The heatmap of key histopathologic findings in lung specimens of study subjects is demonstrated in Fig. 2. In most of the patients (20/25 patients, 80 %), microscopic examination revealed various stages of diffuse alveolar damage, including the exudative phase with hyaline membrane formation (Fig. 3A), the proliferative phase with type 2 pneumocyte hyperplasia (Fig. 3B), and the early repair phase with interstitial spindle cell hyperplasia and/or intraalveolar organization (Fig. 3C). In two of these patients, intraalveolar fibrin balls (Fig. 3D) with minimal hyaline membrane formation and focal intraalveolar organization were seen, which resembled the acute fibrinous and organizing pneumonia (AFOP) pattern (Fig. 3E). Two cases exhibited diffuse alveolar hemorrhage (Fig. 3F), and two necropsy specimens showed near normal lung tissue with scant and focal interstitial and intracapillary aggregation of polymorphonuclear leukocytes (PMNs) (Fig. 3G).

In addition, 15/25 patients (60 %) showed evidence of thrombotic
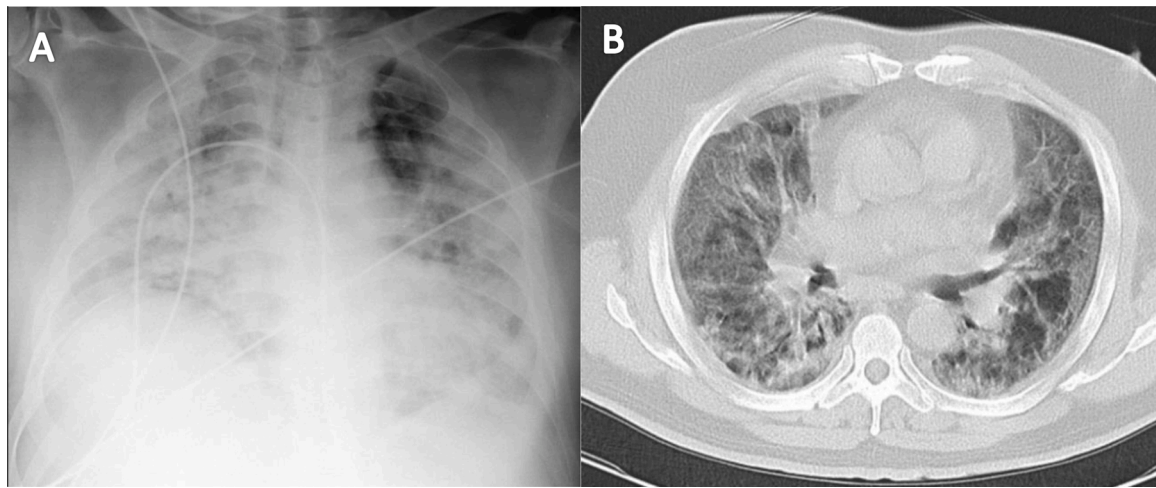
Fig. 1. Antemortem chest x-ray and computed tomography scan of a deceased patient.
A. Cardiomegaly is seen with bilateral peripheral alveolar opacities that mimic reverse batwing sign, simulating acute respiratory distress syndrome (ARDS), B. Axial CT image shows peripheral and symmetrical subpleural ground glass opacities in both lungs.

Table 1
Laboratory findings of decedents.

Variable	Normal range	Value
Blood routine		
WBC, $\times 10^3$ /μl	4–11	9.4 (5.7–13.0)
Hb, g/dl	F: 12.3–15.3; M: 14-17	14 (12–15)
PLT, $\times 10^3$ /μl	150–450	187 (147–296)
Neutrophil		
Percentage, %	34- 59	82 (74–88)
Count, /μl	1800–7700	7600 (4630–11530)
Lymphocyte		
Percentage, %	22- 44	11 (6–17)
Count, /μl	1000–4800	870 (730–1350)
Eosinophil		
Percentage, %	1– 2.7	0.3 (0.1–0.7)
Count, /μl	0–400	28 (10–57)
Blood chemistry		
Urea, mg/dl	F: 15–40; M: 19–44	46 (36–91)
Creatinine, mg/dl	0.7–1.4	1.3 (1.1–1.4)
AST, U/lit	F: 0–37; M: 0–31	52 (37–82)
ALT, U/lit	F: 0–31; M: 0–41	44 (23–62)
ALP, U/lit	64–306	220 (144–281)
Bilirubin, mg/dl		
Total	0.1–1.2	0.8 (0.7–1.8)
Direct	0–0.4	0.8 (0.6–1.1)
LDH, U/lit	up to 480	690 (566–1067)
CPK, U/lit	39–308	140 (66–549)
Albumin, g/dL	3.5–5.2	2.9 ± 0.5
Total protein, g/dl	6.0–8.3	5.6 ± 0.8
Coagulation function		
PT, s	up to 12.9	13.7 (12.8–15.1)
INR	0.9–1.0	1.30 (1.14–1.57)
PTT, s	25–45	45 (39–50)
D-dimer, ng/ml	0–500	9414 ± 7092
Fibrinogen, g/lit	0.4–0.8	3.0 ± 2.7
Infection-related markers		
ESR, mm/h	F: up to 30; M: up to 20	71 ± 35
IL-6, pg/ml	up to 5.9	10.4 (3.2–24.3)
Ferritin, ng/ml	22-275	1813 ± 589
Quantitative CRP, mg/lit	up to 10	52 (23–55)

Data are reported as median (IQR) and mean (± SD).
WBC, white blood cell; Hb, hemoglobin; PLT, platelet; LDH, lactate dehydrogenase; AST, aspartate aminotransferase; ALT, alanine aminotransferase; ALP, alkaline phosphatase; CPK, Creatine phosphokinase; ESR, erythrocyte sedimentation rate; CRP, C-reactive protein; PT, prothrombin time; INR, international normalized ratio; PTT, partial thromboplastin time; IL-6, interleukin-6; F, female; M, male.

Table 2
Results of RT-PCR assay for SARS-CoV-2 in collected samples.

Specimen	Frequency (n/ N)	Percent
Positive nasopharyngeal swab	28/31	90
Positive lung tissue	23/25	92
Positive liver tissue	10/27	37
Positive lung and liver tissue	9/20	45
Positive lung tissue despite negative nasopharyngeal swab	3/25	12

microangiopathy, including capillary, arteriolar or venous thrombus formation (Fig. 3H & I). Hemorrhagic pulmonary infarction was seen in two cases (Fig. 3J). Alveolar edema was the sole histologic manifestation in one patient, while this histologic change was accompanied by other significant histopathologic findings in three other patients (Fig. 3K). Mild to moderate predominantly interstitial and also intraalveolar mononuclear inflammatory cells were also seen in several patients. There was evidence of bronchopneumonic changes in seven cases (28 %) (Fig. 3L), five of whom showed overlapping features of exudative, proliferative, and early repair phase of diffuse alveolar damage along with extensive hyaline membrane formation in the same biopsy specimen. Five patients had areas of collagenous fibrosis highlighted by Masson trichrome staining (Fig. 3M) in addition to aggregation of black dust-laden macrophages associated with few anthracotic nodules. Several specimens, especially those showing the proliferative phase of diffuse alveolar damage, exhibited varying numbers of large atypical cells; some with prominent nucleoli, a few with intracytoplasmic eosinophilic or pale pink inclusions (Fig. 3N), and a few with cytoplasmic vacuoles (Fig. 3O), or syncytial cells with overlapping to convoluted nuclei (Fig. 3P). Also, several alveolar lining cells with smudged hyperchromatic nuclei (Fig. 3Q) as well as increased pulmonary intracapillary megakaryocytes (Fig. 3R) were found on microscopic examination. There was evidence of small airway (terminal bronchiolar) damage accompanied by bronchiolarization (bronchial metaplasia) of adjacent alveolar spaces in two patients. Despite thorough complementary studies with special stains (PAS, Gomori methenamine silver, Gram and Ziehl-Neelsen), no causative agent was identified. Detailed information about the main histopathologic findings of lung tissue samples and stages of diffuse alveolar damage observed in each individual case is available in Supplementary file 1.
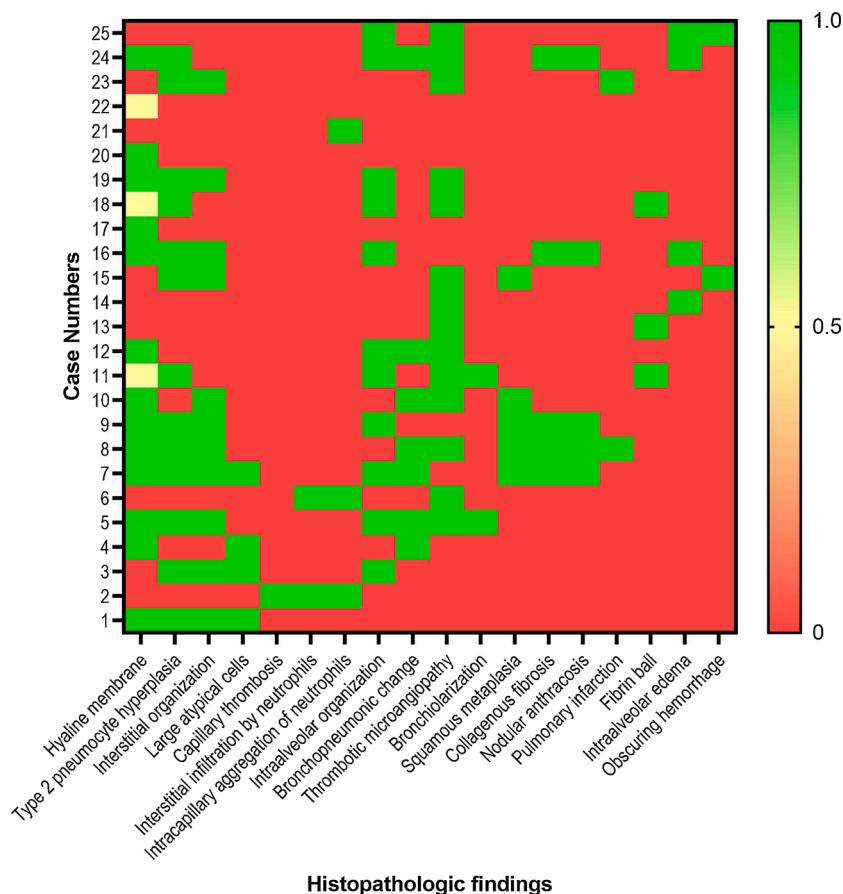
Fig. 2. Heatmap of key histopathologic findings in lung specimens of study subjects.
Value 1 indicates present, 0.5 indicates minimal, and 0 indicates absent pathology.

3.4.2. Liver

Totally, 16/27 liver biopsy specimens (59 %) showed fatty changes that were predominantly macrovesicular steatosis; however, some specimens showed a mixed macro-microvesicular pattern and two specimens had a predominant microvesicular pattern of involvement. Mild to severe portal lymphoplasmacytic inflammation was present in 16 cases (59 %), some with interface hepatitis, and 19 cases (70 %) showed passive congestion. Hepatocellular injury and lobular inflammation were variably seen in some of the liver tissue specimens. Two cases (7 %) showed extensive parenchymal brown-colored pigmentation that failed to stain with Perls but were faintly PAS-positive, being more in favor of lipofuscin granules than bile stasis. Also, examination of one specimen (4 %) revealed multifocal parenchymal necrosis with suspicious intracytoplasmic inclusions.

4. Discussion

Acute lung injury can be caused by a vast range of insults, including infection. Infectious agents, especially viruses, can produce diffuse alveolar damage, a non-specific response of the lung to injury, regardless of the underlying etiology. The microscopic features of diffuse alveolar damage, which are determined by the time interval from injury to biopsy as well as the severity of the injury, appear in a chronological order, demonstrated by an early exudative phase, a subacute proliferative phase and a late repair phase; various phases that greatly overlap one another [14,15].

Based on the results of this study, histopathologic analysis of deceased patients infected with SARS-CoV-2 showed that the majority of lung specimens (80 %) exhibited diffuse alveolar damage. Different phases of diffuse alveolar damage were observed, including the

exudative, proliferative, and early repair phase. This histological pattern was characterized by hyaline membrane formation, type 2 pneumocyte hyperplasia, intraalveolar organization and interstitial spindle cell hyperplasia. Moreover, the AFOP pattern seen in two patients, which was also described by Hwang et al. [16], could be assumed as a pattern within the histologic spectrum of diffuse alveolar damage, representing a fibrinous variant of diffuse alveolar damage [15]. Pathology studies from previous MERS and SARS pandemics also demonstrated that diffuse alveolar damage and AFOP were the predominant postmortem findings in lung specimens of infected patients [16,17]. Therefore, according to findings of our study and other published studies [18–20], the histopathologic findings as well as the clinical manifestations of COVID-19 seem to be similar to those found in SARS and MERS. Nevertheless, it is worthy to note that Magro and colleagues reported that diffuse alveolar damage was not a prominent finding in patients with severe COVID-19 [21]. They declared that the pathophysiology of COVID-19 might not be similar to that of a typical ARDS.

Generally, diffuse alveolar damage is considered as the histopathologic hallmark of ARDS. Several studies, however, have indicated that not all patients with a clinical diagnosis of ARDS manifest findings suggestive of diffuse alveolar damage at histopathological examination [22]. In fact, the presence of diffuse alveolar damage among patients with ARDS contributes to worse clinical outcomes compared with those without diffuse alveolar damage [23,24]. This might also have therapeutic implications, since targeted therapies could be developed against specific cellular and molecular mechanisms of diffuse alveolar damage in this subpopulation of patients with ARDS [25]. Given that effective treatments are still lacking for patients with COVID-19, such clinicopathologic findings could prove to be beneficial for patient management. Nevertheless, identifying COVID-19 patients with diffuse alveolar
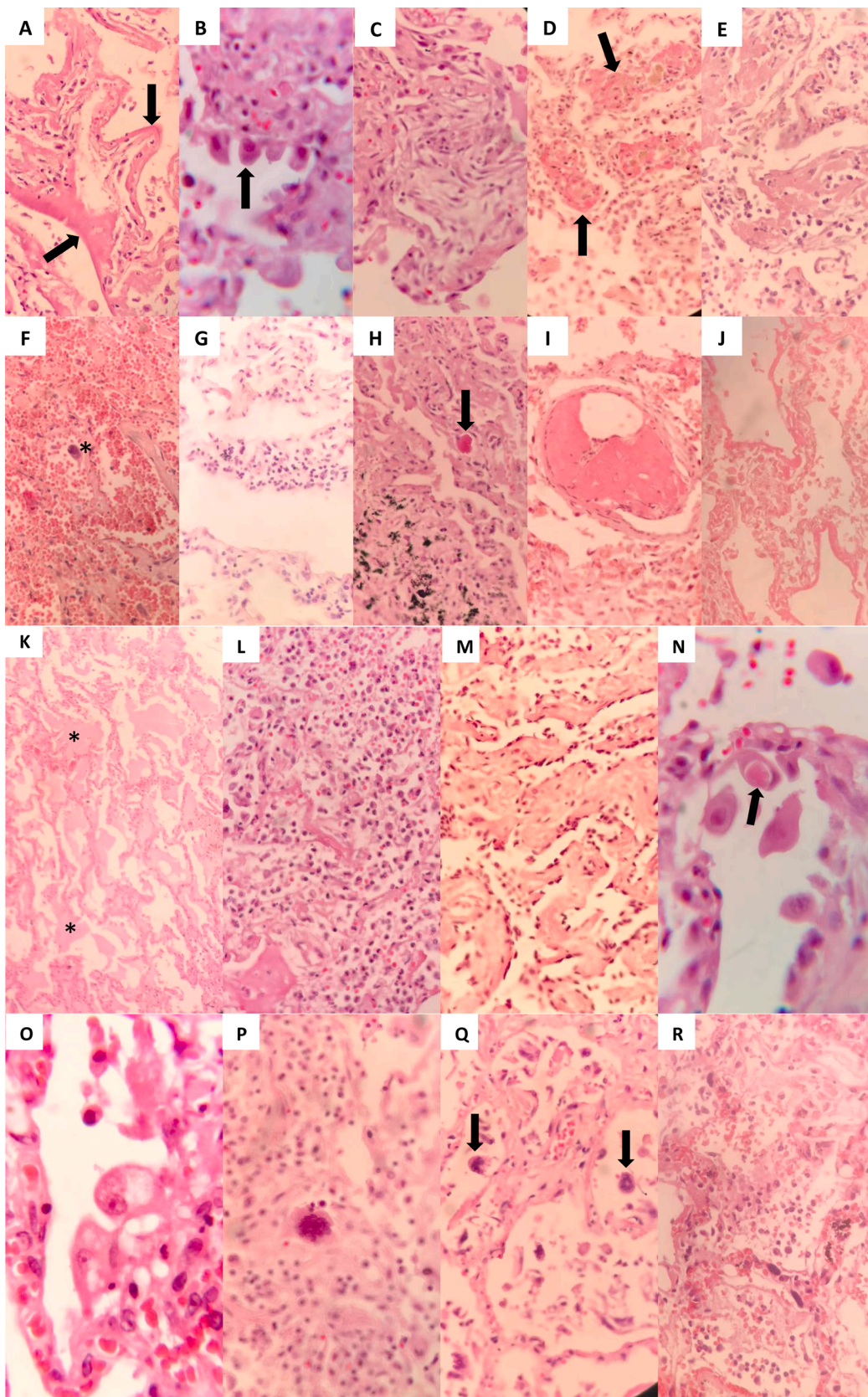
Fig. 3. Histopathologic findings in lung biopsy specimens.

A. Exudative phase of diffuse alveolar damage with prominent hyaline membrane formation (black arrows), B. Proliferative phase of diffuse alveolar damage with prominent type 2 pneumocyte hyperplasia (black arrow), C. Intraalveolar organization (late proliferative to early repair phase), D. Intra-alveolar fibrin balls (black arrows) with focal organization, E. Acute fibrinous and organizing pneumonia pattern, F. Diffuse obscuring alveolar hemorrhage; note the included binucleated cell with hyperchromatic nucleus (asterisk), G. Interstitial and intracapillary neutrophil accumulation, H. Microvascular thrombosis as a component of microangiopathy (black arrow), I. Organized thrombus in a small pulmonary vessel, J. Parenchymal infarction; note the included hyaline membranes. K. Alveolar edema and capillary congestion in early exudative phase (asterisks), L. Suppurative bronchopneumonic changes; note alveolar spaces filled with neutrophils, M. Areas of interstitial thickening by collagenous fibrosis, N. Alveolar lining cell with intracytoplasmic inclusion of unknown nature (black arrow), O. Alveolar lining cell with cytoplasmic vacuolation and a small eosinophilic inclusion, P. Syncytial cells with multiple irregular to overlapping nuclei, Q. Cells with smudged hyperchromatic nuclei (black arrows), R. Increased intracapillary megakaryocytes.

damage through noninvasive techniques is a challenging issue in this regard.

Another frequent histopathologic finding in lung specimens was thrombotic microangiopathy, which was observed in 60 % of the cases. Similarly, other studies found that vascular microthrombi is a main pathologic finding in the lung samples of patients infected with SARS-CoV-2, justifying the severe hypoxemia found in critical cases of COVID-19 with minor radiological abnormalities on imaging [26,21, 27]. This was also supported by the observation of PMNs lodged in capillaries of two cases with near normal lung tissue in our study, which might suggest early stage capillaritis.

Cytologic atypia in areas with squamous metaplasia and pneumocyte hyperplasia is a common finding in the proliferative phase of diffuse alveolar damage, regardless of the cause of injury [28]. In our study, large atypical cells with prominent nucleoli, and also other pathologic findings such as smudged nuclei, occasional intracytoplasmic inclusions and cytoplasmic vacuoles were observed in some of the specimens; however, further immunohistochemistry (IHC) and electron microscopy (EM) studies are needed to verify whether these features are indicative of cytopathic or non-cytopathic changes. Other studies have reported that these morphologic changes are apparent, but not confirmed, viral cytopathic effects [18,29,27].

Suppurative bronchopneumonic changes were detected in seven cases of our study, all of whom had a relatively prolonged hospitalization (more than 15 days). This pathologic finding most likely corresponds to a superimposed bacterial infection. Secondary bacterial infections are present in about 15 % of patients with COVID-19, as shown in a recent meta-analysis by Langford et al. [30]. Furthermore, we speculate that the presence of collagenous fibrosis in some patients, stained with Masson trichrome, and marked anthracotic pigment deposition within the lung parenchyma are probably related to the patients' previous occupational or environmental exposure rather than a sign of viral-induced interstitial fibrosis, which was mentioned by Luo et al. [31].

More recently, few studies have used ancillary techniques, such as EM and IHC, to detect coronavirus-like particles in major organs, including the lungs. In a case series by Bradley et al., IHC staining for SARS-CoV-2 spike protein was performed on lung tissues of four patients, all of which showed focal positive results. Also, viral particles were detected in the lung of two patients by EM [32]. Another study reported the presence of SARS-CoV-2 in the endothelial cells located within the lungs, supporting the hypothesis of direct viral-induced endothelial injury [33]. Indeed, as highlighted by Goldsmith and colleagues, several cytoplasmic structures may be misinterpreted as viral-like particles on EM, especially in the context of postmortem sampling [34].

To date, pathologic evaluation of COVID-19 has mainly focused on cardiopulmonary findings; however, several histopathologic reports of other organs are available in the literature. In keeping with the reported literature [35,36], the most frequently observed finding in liver biopsy specimens was passive congestion (70 %), followed by fatty changes (mainly macrovesicular steatosis) and portal lymphoplasmacytic inflammation, which were both seen in approximately 60 % of the patients. However, given that SARS-CoV-2 was only detected in 40 % of tested liver samples and no definitive viral inclusions were detected, the histopathologic changes observed in liver tissue samples might not be a direct effect of the viral pathogen itself. Further studies are needed to define the presence of viral inclusions in liver samples.

Lastly, it is worthy to emphasize that SARS-CoV-2 RT-PCR obtained from lung tissue samples were positive in patients with negative nasopharyngeal swab tests. This finding might indicate the persistent and continued injury of the viral pathogen to the lungs, as different phases of diffuse alveolar damage were also seen concomitantly in several patients, irrespective of disease stage. Yao and colleagues also reported the detection of SARS-CoV-2 by means of RT-PCR in the lung tissue of a patient with three consecutive negative antemortem nasopharyngeal

swab tests [37]. Furthermore, our study showed that RT-PCR has a relatively high sensitivity for the detection of viral RNA in lung tissues with 92 % of tested samples having a positive result. Previously, Wichmann et al. reported that SARS-CoV-2 RNA was detected by RT-PCR in the lungs of 12/12 patients who died with a diagnosis of COVID-19 [20].

This study has several limitations. First, full autopsies were not performed on deceased patients; although postmortem tissue biopsies could provide helpful information, they might not be representative of all the pathologic changes that have occurred in each decedent. Also, IHC staining and EM examinations were not conducted on tissue samples. We recommend more advanced prospective molecular and IHC studies to assess various cytokines responsible for the proposed maladaptive immune responses in patients with COVID-19. In addition, due to incomplete medical records, the cause of death was not reported for patients of this study.

5. Conclusion

Conclusively, postmortem evaluation of lung specimens of fatal cases of COVID-19 mainly showed diffuse alveolar damage and thrombotic microangiopathy as well as bronchopneumonic changes in several patients. With the growing body of evidence on postmortem findings, the pathologic spectrum of COVID-19 will rapidly expand and insights into the pathogenesis and pathophysiology of COVID-19 will aid in the development of more effective treatment strategies. Further studies are needed to investigate whether SARS-CoV-2 directly targets major organs of the human body.

CRediT authorship contribution statement

Farahnaz Sadegh Beigee: Writing - original draft, Conceptualization, Data curation, Investigation. **Mihan Pourabdollah Toutkaboni:** Writing - review & editing, Supervision, Validation, Data curation. **Neda Khalili:** Writing - original draft, Validation, Data curation. **Seyed Alireza Nadji:** Writing - review & editing, Validation, Data curation. **Atosa Dorudinia:** Writing - review & editing, Validation, Data curation. **Mitra Rezaei:** Writing - review & editing, Validation, Data curation. **Elham Askari:** Writing - review & editing, Validation, Data curation. **Behrooz Farzanegan:** Writing - review & editing, Resources. **Majid Marjani:** Writing - review & editing, Resources. **Amir Rafiezadeh:** Writing - review & editing, Resources.

Declaration of Competing Interest

The authors declare that they have no known competing financial interests or personal relationships that could have appeared to influence the work reported in this paper.

Appendix A. Supplementary data

Supplementary material related to this article can be found, in the online version, at doi:https://doi.org/10.1016/j.prp.2020.153228.

References

[1] World Health Organization (WHO), Coronavirus Disease (COVID-2019) Situation Report – 202, 2020. Accessed 9 August 2020, https://www.who.int/emergencies/diseases/novel-coronavirus-2019/situation-reports.

[2] C. Huang, Y. Wang, X. Li, L. Ren, J. Zhao, Y. Hu, et al., Clinical features of patients infected with 2019 novel coronavirus in Wuhan, China, Lancet (2020) 395.

[3] W. Guan, Z. Ni, Y. Hu, W. Liang, C. Ou, J. He, et al., Clinical characteristics of coronavirus disease 2019 in China, N. Engl. J. Med. 382 (2020) 1708–1720.

[4] M. Raoufi, S. Khalili, M. Mansouri, A. Mahdavi, N. Khalili, Well-controlled vs poorly-controlled diabetes in patients with COVID-19: Are there any differences in outcomes and imaging findings? Diabetes Res. Clin. Pract. (2020) 166.

[5] X. Yang, Y. Yu, J. Xu, H. Shu, H. Liu, Y. Wu, et al., Clinical course and outcomes of critically ill patients with SARS-CoV-2 pneumonia in Wuhan, China: a single-centered, retrospective, observational study, Lancet Respir. Med. 8 (2020) 475–481.

[6] M. Carbone, J.B. Green, E.M. Bucci, J.A. Lednicky, Coronaviruses: facts, myths, and hypotheses, J. Thoracic Oncol. 15 (5) (2020) 675–678.

[7] M. Madjid, P. Safavi-Naeini, S.D. Solomon, O. Vardeny, Potential effects of coronaviruses on the cardiovascular system: a review, JAMA Cardiol. 5 (2020) 831–840.

[8] B.M. Henry, M.H.S. De Oliveira, S. Benoit, M. Plebani, G. Lippi, Hematologic, biochemical and immune biomarker abnormalities associated with severe illness and mortality in coronavirus disease 2019 (COVID-19): a meta-analysis, Clin. Chem. Lab. Med. 58 (7) (2020) 1021–1028.

[9] N. Chen, M. Zhou, X. Dong, J. Qu, F. Gong, Y. Han, et al., Epidemiological and clinical characteristics of 99 cases of 2019 novel coronavirus pneumonia in Wuhan, China: a descriptive study, Lancet 395 (10223) (2020) 507–513.

[10] N. Zhu, D. Zhang, W. Wang, X. Li, B. Yang, J. Song, et al., A Novel Coronavirus from Patients with Pneumonia in China, 2019, N. Engl. J. Med. 382 (8) (2020) 727–733.

[11] S. Tian, Y. Xiong, H. Liu, L. Niu, J. Guo, M. Liao, et al., Pathological study of the 2019 novel coronavirus disease (COVID-19) through postmortem core biopsies, Mod. Pathol. 33 (6) (2020) 1007–1014.

[12] S. Salehi, A. Abedi, S. Balakrishnan, A. Gholamrezanezhad, Coronavirus disease 2019 (COVID-19): a systematic review of imaging findings in 919 patients, Am. J. Roentgenol. (2020) 1–7.

[13] V.M. Corman, O. Landt, M. Kaiser, R. Molenkamp, A. Meijer, D.K. Chu, et al., Detection of 2019 novel coronavirus (2019-nCoV) by real-time RT-PCR, Euro Surveill. 25 (3) (2020), 2000045.

[14] B. Corrin, A. Nicholson, Pathology of the Lungs, 3rd ed., Churchill Livingstone, 2011.

[15] O.-Y. Cheung, P. Graziano, M.L. Smith, Acute lung injury, in: K.O. Leslie, M. R. Wick (Eds.), Practical Pulmonary Pathology: A Diagnostic Approach, 3rd ed, Elsevier, 2018, pp. 125–146, e3.

[16] D.M. Hwang, D.W. Chamberlain, S.M. Poutanen, D.E. Low, S.L. Asa, J. Butany, Pulmonary pathology of severe acute respiratory syndrome in Toronto, Mod. Pathol. 18 (1) (2005) 1–10.

[17] K.O. Alsaad, A.H. Hajeer, M. Al Balwi, M. Al Moaiqel, N. Al Oudah, A. Al Ajlan, et al., Histopathology of Middle East respiratory syndrome coronovirus (MERS-CoV) infection - clinicopathological and ultrastructural study, Histopathology 72 (3) (2018) 516–524.

[18] Z. Xu, L. Shi, Y. Wang, J. Zhang, L. Huang, C. Zhang, et al., Pathological findings of COVID-19 associated with acute respiratory distress syndrome, Lancet Respir. Med. 8 (4) (2020) 420–422.

[19] C. Edler, A.S. Schröder, M. Aepfelbacher, A. Fitzek, A. Heinemann, F. Heinrich, et al., Dying with SARS-CoV-2 infection-an autopsy study of the first consecutive 80 cases in Hamburg, Germany, Int. J. Legal Med. 134 (4) (2020) 1275–1284.

[20] D. Wichmann, J.P. Sperhake, M. Lütgehetmann, S. Steurer, C. Edler, A. Heinemann, et al., Autopsy findings and venous thromboembolism in patients with COVID-19, Ann. Intern. Med. 173 (2020) 268–277.

[21] C. Magro, J.J. Mulvey, D. Berlin, G. Nuovo, S. Salvatore, J. Harp, et al., Complement associated microvascular injury and thrombosis in the pathogenesis of severe COVID-19 infection: a report of five cases, Transl. Res. 220 (2020) 1–13.

[22] J.A. Lorente, P. Cardinal-Fernández, D. Muñoz, F. Frutos-Vivar, A.W. Thille, C. Jaramillo, et al., Acute respiratory distress syndrome in patients with and without diffuse alveolar damage: an autopsy study, Intensive Care Med. 41 (11) (2015) 1921–1930.

[23] P. Cardinal-Fernandez, G. Ortiz, C.H. Chang, K.C. Kao, E. Bertreau, C. Philipponnet, et al., Predicting the impact of diffuse alveolar damage through open lung biopsy in acute respiratory distress syndrome-the PREDATOR study, J. Clin. Med. 8 (6) (2019).

[24] P. Cardinal-Fernández, E.K. Bajwa, A. Dominguez-Calvo, J.M. Menéndez, L. Papazian, B.T. Thompson, The presence of diffuse alveolar damage on open lung biopsy is associated with mortality in patients with acute respiratory distress syndrome: a systematic review and meta-analysis, Chest 149 (5) (2016) 1155–1164.

[25] P. Cardinal-Fernández, J.A. Lorente, A. Ballén-Barragán, G. Matute-Bello, Acute respiratory distress syndrome and diffuse alveolar damage. New insights on a complex relationship, Ann. Am. Thorac. Soc. 14 (6) (2017) 844–850.

[26] L. Carsana, A. Sonzogni, A. Nasr, R.S. Rossi, A. Pellegrinelli, P. Zerbi, et al., Pulmonary post-mortem findings in a series of COVID-19 cases from northern Italy: a two-centre descriptive study, Lancet Infect. Dis. (2020).

[27] S.E. Fox, A. Akmatbekov, J.L. Harbert, G. Li, J. Quincy Brown, R.S. Vander Heide, Pulmonary and cardiac pathology in African American patients with COVID-19: an autopsy series from New Orleans, Lancet Respir. Med. 8 (7) (2020) 681–686.

[28] A.-L.A. Katzenstein, Diagnostic Atlas of Non-Neoplastic Lung Disease A Practical Guide for Surgical Pathologists, Springer Publishing, 2016.

[29] C. Suess, R. Hausmann, Gross and histopathological pulmonary findings in a COVID-19 associated death during self-isolation, Int. J. Legal Med. 134 (4) (2020) 1285–1290.

[30] B.J. Langford, M. So, S. Raybardhan, V. Leung, D. Westwood, D.R. MacFadden, et al., Bacterial co-infection and secondary infection in patients with COVID-19: a living rapid review and meta-analysis, Clin. Microbiol. Infect. (2020).

[31] W.Y.H. Luo, J. Gou, X. Li, Y. Sun, J. Li, L. Liu, Clinical Pathology of Critical Patient with Novel Coronavirus Pneumonia (COVID-19), 2020. Preprints, 2020020407.

[32] B.T. Bradley, H. Maioli, R. Johnston, I. Chaudhry, S.L. Fink, H. Xu, et al., Histopathology and ultrastructural findings of fatal COVID-19 infections in Washington State: a case series, Lancet 396 (10247) (2020) 320–332.

[33] M. Ackermann, S.E. Verleden, M. Kuehnel, A. Haverich, T. Welte, F. Laenger, et al., Pulmonary vascular endothelialitis, thrombosis, and angiogenesis in Covid-19, N. Engl. J. Med. 383 (2) (2020) 120–128.

[34] C.S. Goldsmith, S.E. Miller, R.B. Martines, H.A. Bullock, S.R. Zaki, Electron microscopy of SARS-CoV-2: a challenging task, Lancet 395 (10238) (2020) e99.

[35] W.O. Vasquez-Bonilla, R. Orozco, V. Argueta, M. Sierra, L.I. Zambrano, F. Muñoz-Lara, et al., A review of the main histopathological findings in coronavirus disease 2019, Hum. Pathol. (2020).

[36] L.M. Buja, D.A. Wolf, B. Zhao, B. Akkanti, M. McDonald, L. Lelenwa, et al., The emerging spectrum of cardiopulmonary pathology of the coronavirus disease 2019 (COVID-19): report of 3 autopsies from Houston, Texas, and review of autopsy findings from other United States cities, Cardiovasc. Pathol. 48 (2020), 107233.

[37] X.-H. Yao, Z.-C. He, T.-Y. Li, H.-R. Zhang, Y. Wang, H. Mou, et al., Pathological evidence for residual SARS-CoV-2 in pulmonary tissues of a ready-for-discharge patient, Cell Res. 30 (6) (2020) 541–543.

[38] A. Abrishami, et al., Clinical and Radiologic Characteristics of COVID-19 in Patients With CKD, Iranian journal of kidney diseases 14 (4) (2020) 267–277.

[39] S. Haseli, et al., Lobar Distribution of COVID-19 Pneumonia Based on Chest Computed Tomography Findings; A Retrospective Study, Arch Acad Emerg Med 8 (1) (2020).